Spectral purity transfer with 5 × 10−17 instability at 1 s using a multibranch Er:fiber frequency comb

Metrologia

Spectral purity transfer with 5×10^{-17} instability at 1 s using a multibranch Er:fiber frequency comb

OPEN ACCESS
IOP Publishing
Metrologia

Metrologia **56** (2019) 045008 (8pp)
https://doi.org/10.1088/1681-7575/ab2b0f

Spectral purity transfer with 5×10^{-17} instability at 1 s using a multibranch Er:fiber frequency comb

Piero Barbieri[1,2], Cecilia Clivati[1], Marco Pizzocaro[1], Filippo Levi[1] and Davide Calonico[1]

[1] Istituto Nazionale di Ricerca Metrologica-INRIM, Strada delle Cacce 91, 10135 Turin, Italy
[2] Politecnico di Torino, c.so Duca degli Abruzzi 24, 10129 Turin, Italy

E-mail: c.clivati@inrim.it

Received 22 December 2018, revised 19 June 2019
Accepted for publication 19 June 2019
Published 5 July 2019

Abstract

In this work we describe the spectral purity transfer between a 1156 nm ultrastable laser and a 1542 nm diode laser by means of an Er:fiber multibranch comb. By using both the master laser light at 1156 nm and its second-harmonic at 578 nm, together with the 1542 nm slave laser, we investigate the residual noise between the main comb output, the octave-spanning output, and a wavelength conversion module including non-linear fibers, second-harmonic generation crystal and amplifiers. With an ultimate stability of the system at the level of 5×10^{-17} at 1 s and accuracy of 3×10^{-19}, this configuration can sustain spectral transfer at the level required by the contemporary optical clocks with a simple and robust setup.

Keywords: optical frequency comb, multibranch Er:fiber comb, spectral purity transfer, ultrastable laser

(Some figures may appear in colour only in the online journal)

1. Introduction

In the last two decades, optical combs became a fundamental tool in experimental physics, finding applications beyond optical [1, 2] and microwave [3] frequency metrology. Featuring an equidistant series of narrow-linewidth optical modes that covers a broad wavelength range, the comb structure has been exploited in a number of ways to perform precision spectroscopy [4]. The comb can be used as a bridge to transfer traceability to the international system of units (SI) second through different spectral domains, ranging from the UV to the mid-IR. This makes it a key tool in the absolute spectroscopy of atoms and molecules [5, 6]. Atomic and molecular samples can also be directly interrogated over a broad spectral range at a single time through direct comb spectroscopy [7] and dual-comb spectroscopy [8]. Moreover, optical combs allow low-noise frequency synthesis [9] when used as optical frequency dividers. More recently, they found application in astronomy to provide high-resolution calibration for spectrographs [10].

The possibility of transferring the spectral purity of an ultrastable laser across different regions of the optical domain [11–16] is beneficial to the increasing requirement of high frequency stability lasers for optical atomic clocks and high-resolution spectroscopy. Ultrastable lasers are realized using high-finesse optical cavities as frequency reference. In the infrared domain the best cavities achieve the 10^{-17} level of frequency instability exploiting cryogenic environments, long cavity lengths and special mirror coatings [17–19]. The optical comb enables such performances to be copied to any laser in the optical domain, with a simplification of the experimental setup. This is especially relevant when several ultrastable lasers at different wavelengths are needed, where a single ultrastable cavity has to be realized. In this way, not only optical combs improve clock lasers, but also allow high-resolution inter-species optical clocks comparisons [1, 20].

Benefits range from the search for new physics, to more ponderate considerations on the redefinition of the second in the SI, and future computations of the international atomic time based on optical clocks [21, 22].

In recent years, solid-state optical combs have been almost ubiquitously replaced by erbium-doped fiber (Er:fiber) devices. This is due to their higher reliability and robustness, which allow several days of continuous operation. However, their natural emission is in the 1–2 μm region. In order to cover the optical domain, dedicated wavelength conversion modules are exploited. In this way, it is possible to broaden the comb spectrum, preserving the phase-coherence with the fundamental comb and still provide adequate optical power per mode, at the cost of introducing additional noise to the system.

In this paper we present the spectral purity transfer between a 1156 nm ultrastable diode laser and a 1542 nm diode laser performed with an Er:fiber comb. The 1156 nm laser is used, after frequency doubling, as a clock laser in our Yb lattice clock at the Italian Metrology Institute (INRIM) [23]. Spectral transfer to a telecom wavelength will enable us to disseminate the frequency of the Yb standard to a number of research facilities, using the phase-stabilized ∼2000 km optical fiber backbone we developed in Italy [24]. In addition, this setup will be used to generate the clock laser for the Sr optical clock under development in our laboratories [25].

We use the transfer oscillator technique proposed by Telle *et al* [26]. The beatnote between the 1542 nm slave laser and the comb is performed on the main comb output, which spans the 1.5–1.6 μm region. The 1156 nm master laser is detected on the broadband branch that spans the 1–2 μm range. The frequency-doubled master laser at 578 nm is detected on a few nm-wide dedicated branch. By using both the fundamental and frequency-doubled master laser we characterized the spectral transfer and the contribution of the separate comb branches without the need of a second, independent system. This measurement approach, which uses a single comb to study the spectral purity transfer, is different from that presented in previous works. Usually, two independent optical combs are used, one to perform the locking between the master and the slave lasers, the other to detect the out-of-loop beatnote [11–14].

In our work we separately considered all noise contributions to the spectral purity transfer, and we characterized both the electronics and the environmental noise on interferometers independently. We show that an Er:fiber optical comb used in the multibranch configuration achieves a residual frequency instability of $5 \times 10^{-17}(\tau/\mathrm{s})^{-1/2}$ with accuracy of 3×10^{-19}.

Even if single-branch combs achieve better performances [15, 16], a multibranch configuration offers higher power-per-mode in different spectral regions, which simplifies the measurement setup. Very recently, a method for rejecting the inter-branch comb noise has been demonstrated [27], which is promising when ultra high-accuracy has to be guaranteed. However, multibranch configuration still offers adequate performances with a simple and robust system.

2. Experimental setup

2.1. The optical frequency comb

The optical comb used for the spectral purity transfer is a commercial femtosecond Er:fiber comb. It is based on passive mode-locking through non-linear polarization rotation. The main output is centered at 1560 nm and spans 100 nm, the repetition rate f_{rep} is 250 MHz.

The main comb output is split in three independent branches (see figure 1). The first branch is a fraction of the 1560 nm output of the femtosecond mode-locked laser. The second branch consists in an erbium-doped fiber amplifier (EDFA) followed by a highly non-linear fiber (HNLF) that generates an octave-spanning spectrum between 1 μm and 2 μm. This branch is used to detect the carrier-envelope offset frequency f_0 through the $f-2f$ interferometer, with 2.5 mW power output available for other measurements. The third branch is a wavelength conversion module operating at 578 nm. It consists in a second EDFA and a wavelength-shifting fiber that produces 1156 nm radiation. Then, the 1156 nm light is frequency-doubled with a bulk periodically poled lithium niobate (PPLN) crystal. In this way a 1.1 nm-wide output at 578 nm is obtained, with an average power of 5 mW and a power per tooth of 1 μW. The spectrum of the $f-2f$ and the 578 nm branches can be tailored by adjusting the current of the 980 nm pump diode lasers that act on the EDFAs (four pump lasers for each EDFA).

The repetition rate and the offset frequency are stabilized to a hydrogen maser by means of two phase-locked-loops (PLLs). The former acts on the cavity length by moving one of the cavity mirrors using a piezo, on a bandwidth of 3.5 kHz. The second acts on the power of the femtosecond Er:fiber oscillator pump laser to modify intracavity dispersion. In principle, the spectral transfer does not require a tight stabilization of the comb repetition rate and offset frequency, since their noise is canceled out [26]. In practice, however, they are locked to prevent long-term drifts that might bring beatnotes outside the filters' bandwidth.

The comb and all the optical interferometers developed for the beatnotes' detection are placed in a foam enclosure to reduce the effect of air currents and temperature variations on the fiber.

2.2. Laser sources and beatnote detection

The master laser used in our experiment is a 1156 nm diode laser, frequency-doubled in a waveguide-PPLN crystal to 578 nm. This is used to probe the $^1S_0 - {}^3P_0$ clock transition at 578 nm of the ^{171}Yb optical lattice clock [23]. The doubling stage produces up to 9 mW of 578 nm radiation, while 4 mW of 1156 nm are still available after the crystal waveguide. Part of the 578 nm radiation is used to stabilize the laser to a 10 cm cavity made of ultra-low expansion glass through the Pound–Drever–Hall technique [28]. The residual laser frequency instability is 2×10^{-15} at 1 s averaging time, with a drift of 0.15 Hz s^{-1}. 1 mW of the 1156 nm laser is detected on the $f-2f$-branch of the comb. The beatnote reaches up to 37 dB

of signal-to-noise ratio (SNR) in a 100 kHz resolution bandwidth (RBW). 600 μW of 578 nm light are beaten with the 578 nm comb branch, producing a beatnote signal with 35 dB SNR in a 100 kHz RBW. The 1156 nm and 578 nm radiations are sent to the optical comb through polarization-maintaining (PM) Doppler-stabilized optical fibers [29]. Both beatnotes are detected through free-space interferometers. An external cavity diode laser at 1542 nm with output power of 9 mW [30] and linewidth <10 kHz is phase-locked to the master laser at 1156 nm using the transfer oscillator scheme. 100 μW of its output power are beaten to the main comb output at 1560 nm through an all-fiber-coupled optical interferometer. The detected beatnote has a SNR of 40 dB in a 100 kHz RBW.

We use a transfer oscillator scheme to obtain a beatnote between the 1542 nm laser and the 1156 nm laser [26]. This is stabilized by a PLL that acts on an acousto-optic modulator with a bandwidth of 60 kHz, and on the diode laser current. The slave laser is used without any pre-stabilization. Thanks to the high SNR on all beatnotes, we can achieve cycles-slips free operation for several hours with minimal adjustment of the comb amplifiers pump power, and do not need tracking oscillators.

2.3. Transfer oscillator setup

Figure 2 shows the electronic setup we developed for generating the virtual beatnote between the 1156 nm master laser and the 1542 nm slave laser (in-loop beatnote f_{in}), which is used for the PLL.

Being ν_{1156} and ν_{1542} the absolute frequencies of the CW lasers, $f_{\mathrm{b},1156}$ and $f_{\mathrm{b},1542}$ the beatnotes between the CW lasers and the comb, m_{1156} and m_{1542} the indexes of the comb teeth to which the lasers are beaten, then the in-loop beatnote can be written as:

$$\begin{aligned} f_{\mathrm{in}} &= \tfrac{1}{4}\tfrac{m_{1542}}{m_{1156}}\bar{f}_{\mathrm{b},1156} - \tfrac{1}{4}\bar{f}_{\mathrm{b},1542} \\ &= \tfrac{1}{4}\left(\nu_{1542} - \tfrac{m_{1542}}{m_{1156}}\nu_{1156}\right), \end{aligned} \tag{1}$$

where $\bar{f}_{\mathrm{b},1156}$ and $\bar{f}_{\mathrm{b},1542}$ indicate the f_0-free signals $\bar{f}_{\mathrm{b},1156} = f_{\mathrm{b},1156} + f_0$ and $\bar{f}_{\mathrm{b},1542} = f_{\mathrm{b},1542} + f_0$, which are obtained using frequency mixers.

The scaling factor $1/4 \times m_{1542}/m_{1156}$ is applied to $\bar{f}_{\mathrm{b},1156}$ by using a direct digital synthesizer (DDS). The factor of 1/4 is used as with the original teeth ratio $m_{1542}/m_{1156} \simeq 0.75$ the DDS output frequency would be above the DDS Nyquist frequency. A second DDS (DDS2 in figure 2) or a prescaler is used to scale $\bar{f}_{\mathrm{b},1542}$ accordingly. We use Analog Devices AD9912 DDSs, which have a 14-bit digital-to-analog converter and 4 μHz resolution. We verified that the DDSs do not introduce cycles slips as long as the SNR on the beatnotes and on f_0 is >33 dB in a 100 kHz RBW.

The electronic scheme has been designed to be easily adapted to any value of the beatnotes with minor changes. Several local oscillators (LOs) are used to match the band-pass filters and have been omitted in equation (1) for the sake of clarity. The red elements in figure 2 indicate the only components that need to be adjusted when using different lasers, i.e. the frequency of the LOs and the band-pass filters at the output of the DDSs.

3. Characterization

To fully characterize the spectral transfer and the inter-branch noise, we performed the following measurements: first, we characterized the noise between the 1.56 μm-branch, the $f-2f$-branch and the 578 nm-branch. Then, we compared the 1542 nm slave laser, phase-locked to the 1156 nm master laser, to the second harmonic of the latter at 578 nm. Measurements were conducted using a digital phasemeter with 1 MHz bandwidth and an eight-channel, dead-time free synchronous frequency counter in the averaging configuration with 1 s gate time. The two measurement approaches are complementary: the former allowed computation of phase noise spectra, suited to inspect fundamental noise processes at high Fourier frequencies. The latter has been used to calculate the frequency instability in terms of Allan deviation, that better quantifies the long-term behavior of the system. Thanks to the leverage between RF and optical domain, the counter resolution did not limit the measurement at the 2×10^{-20} level.

3.1. f − 2f and 1.56μm branches noise

We detected the beatnotes between the same laser at 1542 nm and the comb in the $f-2f$ and 1.56 μm branches and analyzed the frequency noise of their difference. Figure 3 (green curve) shows the corresponding power spectral density, that quantifies the residual frequency noise between the two branches. The residual instability is shown in terms of overlapping Allan deviation by the green curve in figure 4, which is in agreement with the observed spectrum, considering that the equivalent measurement bandwidth of the counter is 0.5 Hz.

We note that the $f-2f$ branch includes an EDFA and a HNLF to achieve the octave-spanning broadening, while the 1.56 μm branch does not include additional components. Therefore, the reported curves represent the noise of EDFA, HNFL and other uncommon fibers.

3.2. f − 2f and 578 nm branches noise

We measured the frequency ratio between the 1156 nm master laser beaten to the $f-2f$-branch and its 578 nm second harmonic beaten to the 578 nm-branch ($f_{\mathrm{b},578}$). We calculated the virtual beatnote between the two lasers by post-processing the simultaneous counting of f_0, $f_{\mathrm{b},1156}$ and $f_{\mathrm{b},578}$.

For a better inspection of high-frequency noise we also generate this beatnote physically by implementing the transfer oscillator scheme shown in figure 5. Note that if the comb branch used for the beatnote detection is generated from a frequency-doubling process, as in the case of the 578 nm-branch, the second harmonic of f_0 is used to produce the f_0-free beatnote instead of the fundamental tone. This is achieved by adding a multiplier after f_0 ('2×' box in figure 5). Therefore, the f_0-free beatnote in this case is $\bar{f}_{\mathrm{b},578} = f_{\mathrm{b},578} + 2f_0$.

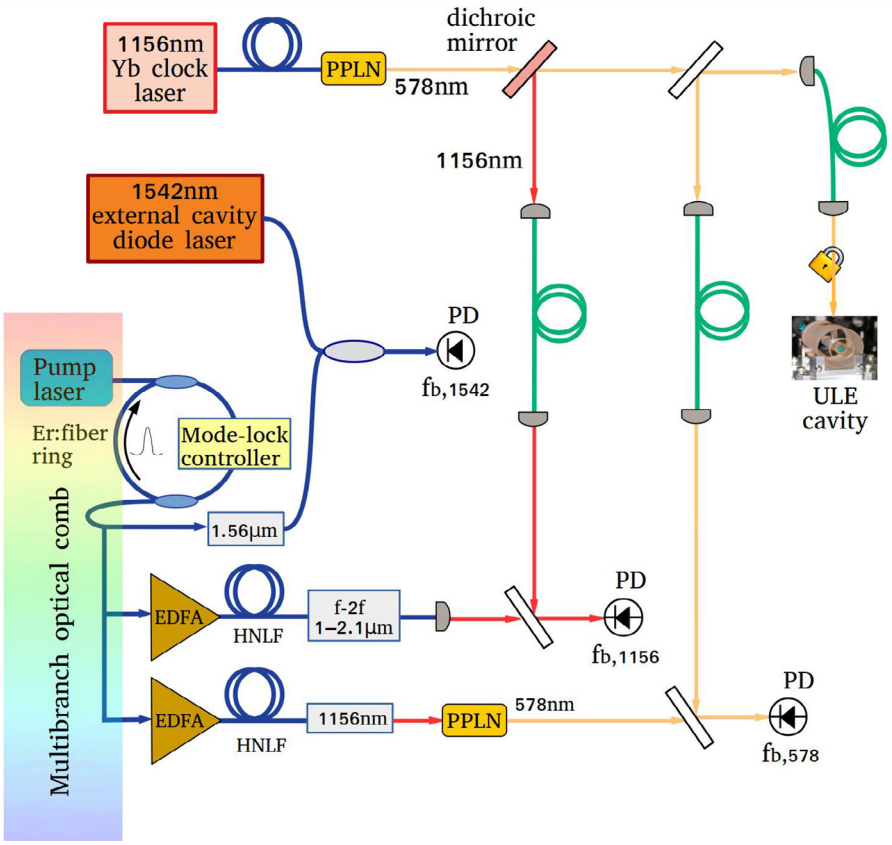

Figure 1. Optical comb and laser beatnote detection setup. The comb main output at 1.56 μm is split into three branches. EDFA: erbium-doped fiber amplifier, HNLF: highly non-linear fiber, PPLN: periodically poled lithium niobate crystal, PD: photodiode. $f_{b,1542}$, $f_{b,1156}$, $f_{b,578}$: beatnotes between the 1542 nm, 1156 nm, 578 nm radiations and the comb. Blue lines: uncompensated fibers, green lines: phase-stabilized fibers, red and yellow lines: free-space paths.

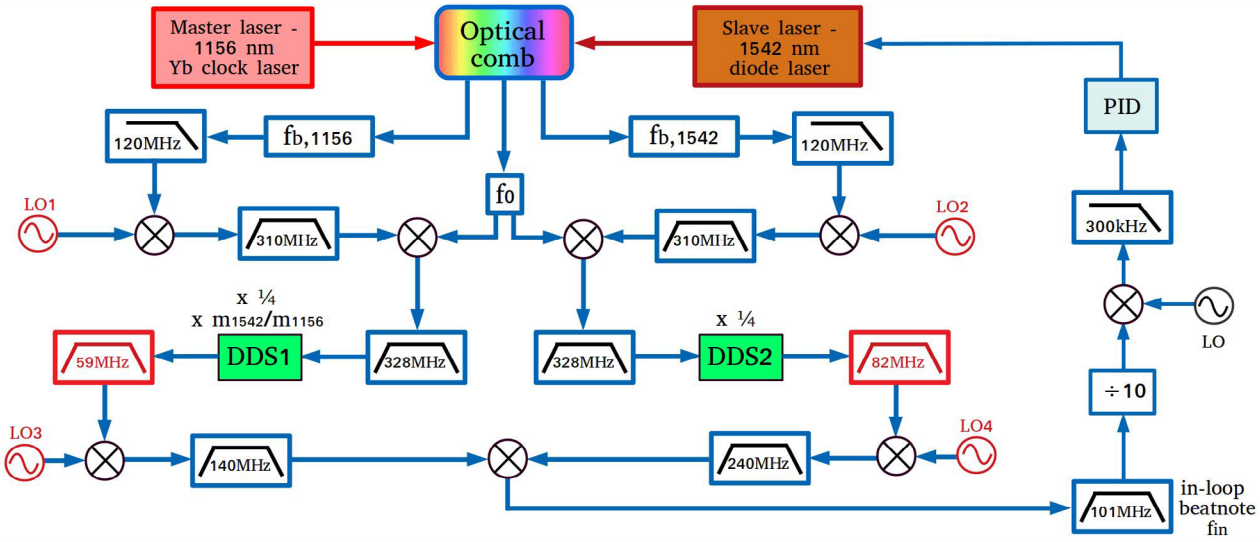

Figure 2. Experimental setup developed for phase-locking the 1542 nm slave laser to the 1156 nm master laser using the transfer oscillator technique. Red: adjustable components of the system. DDS: direct digital synthesizer; ⊗: mixer; LO: local oscillator, PID: proportional-integral-derivative controller.

Figures 3 and 4 show the corresponding frequency noise and instability (yellow curves). In these measurements, both comb outputs are directly combined with the laser light through free-space paths. This configuration leads to a long-term instability dominated by a white frequency noise process for $\tau > 10$ s in agreement with the observed spectrum, and achieves an ultimate level of 3×10^{-19} at 10 000 s. No offset was observed at this level. This puts an upper limit to the frequency instability of conversion between fundamental and second harmonic radiation at 578 nm in our crystal and phase-stabilized fiber links that bring the 1156 nm and the 578 nm light to the comb. We also note that a flicker frequency

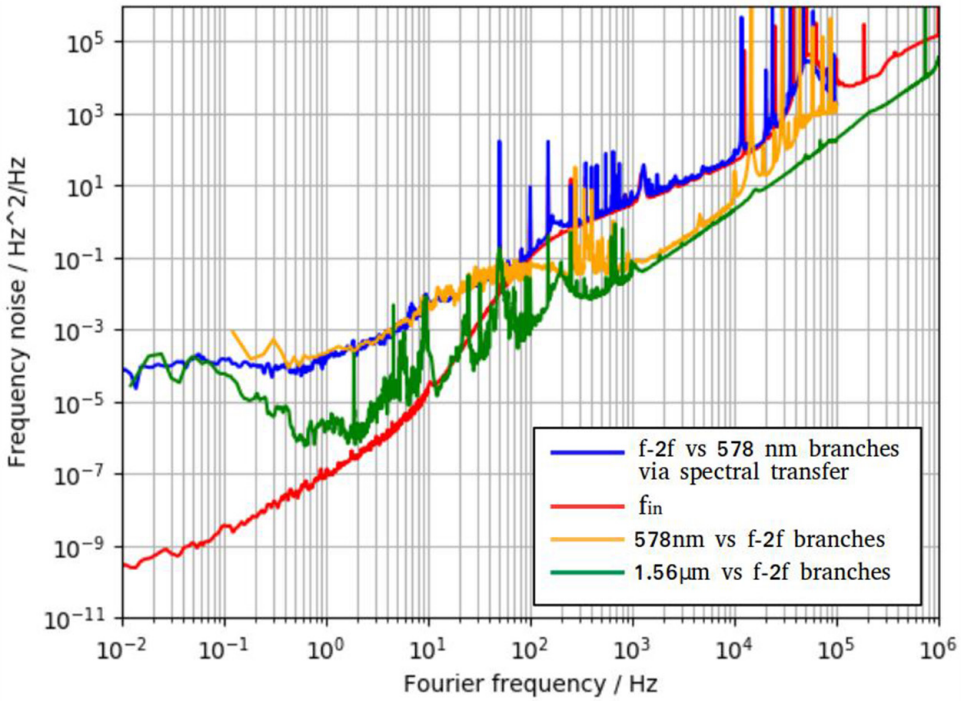

Figure 3. Frequency noise spectrum of the comparison between the $f-2f$ and 578 nm branches via spectral purity transfer at 1542 nm laser (blue), of the in-loop beatnote f_{in} between the 1542 nm laser and the 1156 nm laser (red), of the 578 nm-branch with respect to the to the $f-2f$-branch (yellow), of the 1.56 μm branch with respect to the $f-2f$-branch (green). All the spectra are reported in the 1542 nm spectral window.

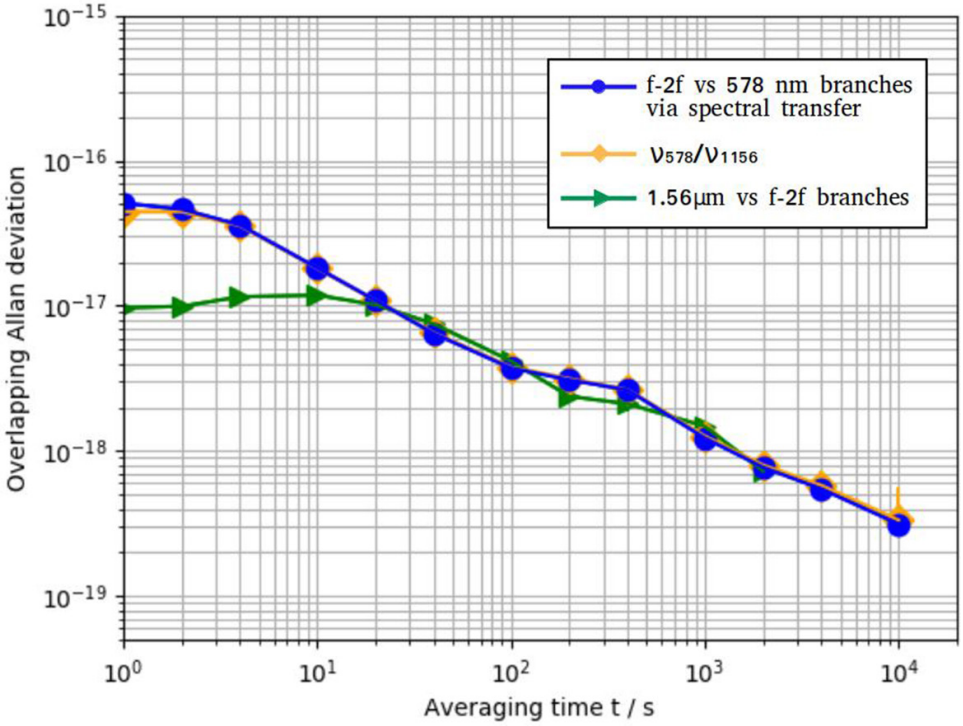

Figure 4. Fractional stability measurements in terms of Allan deviation (Adev). Green: $f-2f$ and 1.56 μm branches noise measured by beating the same 1542 nm laser on the two branches. Blue: $f-2f$ and 578 nm branches noise via spectral purity transfer at 1542 nm. Yellow: frequency ratio measurement ν_{578}/ν_{1156}.

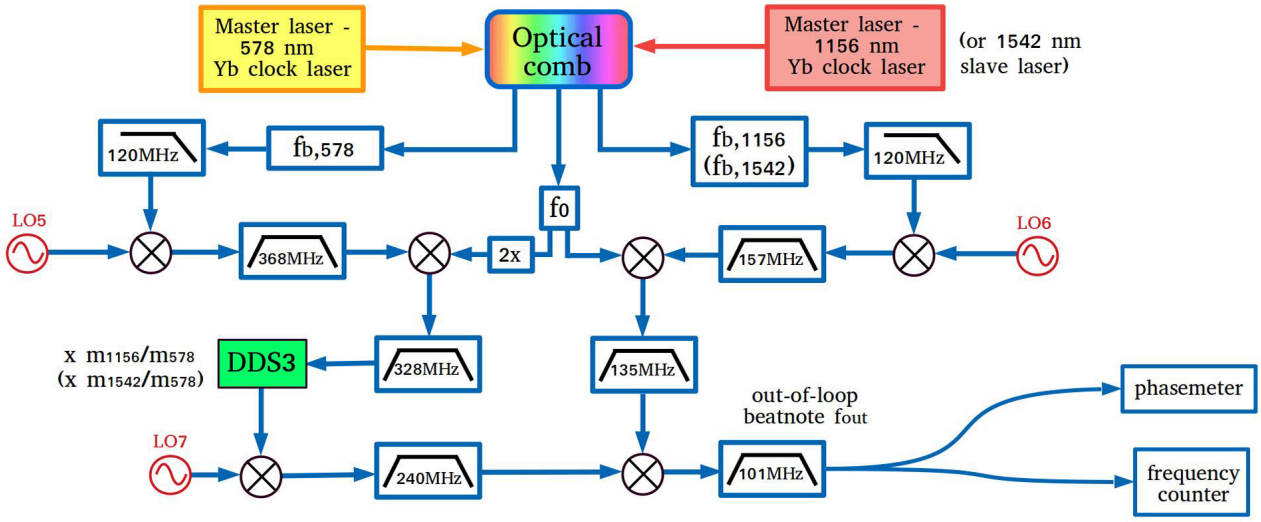

Figure 5. Experimental setup developed for the measurement of the virtual beatnote between the 1156 nm master laser and its 578 nm second harmonic. Red: adjustable components of the system. DDS: direct digital synthesizer; ⊗: mixer; LO: local oscillator. The brackets indicate the characterization of the spectral puirty transfer by analyzing the virtual beatnote between the 1542 nm slave laser and the 578 nm second harmonic of the master laser.

instability at the level of 5×10^{-18} was observed when the $f - 2f$ comb output traveled over a 1 m uncompensated PM fiber. For that reason, we replaced uncompensated fiber paths with free-space paths in our comb wherever possible.

3.3. f − 2f and 578 nm branches via spectral purity transfer at 1542 nm

We measured the virtual beatnote between the 578 nm and the 1542 nm lasers when the latter was phase-locked to the 1156 nm laser. The implementation scheme is shown in figure 5 (see labels in brackets). Figures 3 and 4 show the corresponding frequency noise and instability (blue curves). The Allan deviation achieves the 5×10^{-17} level at 1 s, in agreement with the observed spectrum, and decreases to the ultimate 3×10^{-19} level after 10 000 s. Noise sources that affect this beatnote include the residual noise between the $f - 2f$ and the 578 nm comb branches, the noise of the PLL between the 1542 nm and the 1156 nm laser, the noise of the phase-stabilized fibers which bring the 1156 nm and the 578 nm light to the comb, and possibly the noise of the second harmonic generation at 578 nm. The noise of the 1.56 μm-branch is rejected as it is common between the two transfer schemes.

3.4. Comments

From the measurements described in sections 3.1–3.3, we can quantify the noise of the three branches and the spectral transfer between our 1156 nm and 1542 nm lasers. From a comparison of the spectra in figure 3, it is evident that the measurements involving the 578 nm-branch have a higher noise at Fourier frequencies between 10^{-1} Hz and 100 Hz. This behavior can be seen as well from the comparison of the short term frequency instability of the three measurements. This is attributed to the phase-stabilization circuits that independently stabilize the fibers paths of the 1156 nm and 578 nm lasers to the comb [29]. The performances of the spectral transfer between the 1156 nm and the 1542 nm laser are represented by a combination of the results of the tests described in sections 3.1 and 3.3. The inter-branch noise between the 1.56 μm and $f - 2f$ branches, shown by the green curve in figure 3, quantifies the noise of EDFA, HNLF and other uncompensated fibers. The noise excess corresponding to the slope deviation from white frequency noise below 1 Hz Fourier frequencies is attributed to thermal effects in the laboratory. The blue curve in the figure includes the inter-branch noise between the 578 nm and $f - 2f$ branches and the noise of the PLL as well. As it is dominant over the inter-branch comb throughout the full Fourier spectrum, we can consider it as the upper limit to the spectral transfer noise. At Fourier frequencies >100 Hz, the noise is limited by the in-band rejection of the PLL, hence by the locking bandwidth, as can be noted by comparing the blue curve with respect to the in-loop beatnote f_{in} noise (red curve). Further reduction in the high-frequency noise could be gained with higher bandwidth or with low-noise diode lasers. At lower frequencies, the inter-branch noise emerges. The measurement sensitivity is here limited by the fiber-stabilization loops; the lower limit to the noise is represented by the green curve, i.e. the inter-branch noise between the 1.56 μm and the $f - 2f$ branches. The corresponding fractional frequency instability is 5×10^{-17} at 1 s. We note that a residual sensitivity to the external environment is still observed around 400 s, which is due to the air conditioning in our laboratory. Even in the worst case, however, the ultimate stability achieves the level of 3×10^{-19} and no frequency offset has been observed at this level.

4. Discussion and conclusions

We performed the spectral purity transfer between the 1156 nm ultrastable laser used to probe the clock transition of the ^{171}Yb optical lattice clock and a 1542 nm diode laser,

without any pre-stabilization for the latter. We implemented the transfer oscillator technique using an Er:fiber multibranch frequency comb. Having available both the master laser light at 1156 nm and its 578 nm second harmonic, we characterized the spectral transfer without using a second reference comb. In this way, we put an upper limit to the transfer instability at the $5 \times 10^{-17}(\tau/\mathrm{s})^{-1/2}$ level with an ultimate uncertainty of 3×10^{-19}, limited by the uncorrelated noise between the comb branches. Our multibranch optical comb is adequate for the spectral purity transfer of our ultrastable laser sources, allowing the possibility of Dick-effect-free comparison of our optical clocks [1, 20]. We highlight that the availability of a laser which can be measured on independent comb outputs, directly or by means of a frequency-doubling crystal, allows a direct measurement of the inter-branch noise. Specifically, it can be used to characterize the $f - 2f$ branch with respect to wavelength dedicated modules. In our case, the measurement of a 1542 nm laser on the $f - 2f$ and 1.56 µm branches, and the frequency doubling of a 1156 nm laser, allowed characterization of the uncorrelated noise between the $f - 2f$, 578 nm and the 1.56 µm branches. In addition, the possibility of doubling the master laser's frequency enabled us to put an upper limit to the electronics noise included in the spectral transfer between the 1156 nm and 1542 nm lasers. Still, we stress that such a measurement does not directly characterize the coherence between the comb in the master and slave lasers spectral regions. An indirect evaluation of the upper limit to de-coherence of the full comb comes however from the comparison between the fundamental and doubled master laser's frequency. When non-linear frequency conversion between the various domains is not available, one should rely on absolute frequency measurements on different combs.

Albeit the performances of single-branch frequency combs are superior, with a short-term frequency instability at the 3×10^{-18} level [16], our setup presents some practical advantages. It is easier to implement and more immune to cycles-slips, as the use of dedicated branches ensures higher power per mode and higher SNR at detection in the relevant spectral regions, and independent paths can be used for beatnote detection. In addition, as separate amplifiers are used for each branch, it is easier to tailor the spectrum of the various outputs in order to optimize each beatnote independently. The realized apparatus will be used to disseminate the frequency of our Yb optical clock along the Italian optical fiber link, and to realize the clock laser at 698 nm for our Sr lattice clock under development.

We believe our characterization is general, since the $f - 2f$ interferometer allows measurement of a broad range of frequencies in the 1–2 µm domain. A general scheme for frequency transfer can thus exploit the $f - 2f$-branch for detection of a near-infrared master laser, and a dedicated wavelength conversion module for reaching the spectral region of interest for the experiment. Here, we characterized a module at 578 nm, however the physical components are the same as for other wavelength-dedicated modules.

Acknowledgments

This work has been funded by EMPIR-15SIB03-OC18 and EMPIR-15SIB05-OFTEN, which have received funding from the EMPIR programme co-financed by the Participating States and from the European Union's Horizon 2020 research and innovation programme.

ORCID iDs

Marco Pizzocaro https://orcid.org/0000-0003-2353-362X

References

[1] Nemitz N, Ohkubo T, Takamoto M, Ushijima I, Das M, Ohmae N and Katori H 2016 Frequency ratio of Yb and Sr clocks with 5×10^{-17} uncertainty at 150 s averaging time *Nat. Photon.* **10** 258–61

[2] Grotti J *et al* 2018 Geodesy and metrology with a transportable optical clock *Nat. Phys.* **14** 437–41

[3] Millo J *et al* 2009 Ultralow noise microwave generation with fiber-based optical frequency comb and application to atomic fountain clock *Appl. Phys. Lett.* **94** 141105

[4] Picqué N and Hänsch T W 2019 Frequency comb spectroscopy *Nat. Photon.* **13** 146–57

[5] Clivati C *et al* 2016 Measuring absolute frequencies beyond the GPS limit via long-haul optical frequency dissemination *Opt. Express* **24** 11865–75

[6] Santagata R *et al* 2019 High-precision methanol spectroscopy with a widely tunable SI-traceable frequency-comb-based mid-infrared QCL *Optica* **6** 411–23

[7] Cingöz A, Yost D C, Allison T K, Ruehl A, Fermann M E, Hartl I and Ye J 2012 Direct frequency comb spectroscopy in the extreme ultraviolet *Nature* **482** 68–71

[8] Coddington I, Newbury N and Swann W 2016 Dual-comb spectroscopy *Optica* **3** 414–26

[9] Fortier T M *et al* 2011 Generation of ultrastable microwaves via optical frequency division *Nat. Photon.* **5** 425–9

[10] McCracken R A, Charsley J M and Reid D T 2017 A decade of astrocombs: recent advances in frequency combs for astronomy *Opt. Express* **25** 15058–78

[11] Nakajima Y *et al* 2010 A multi-branch, fiber-based frequency comb with millihertz-level relative linewidths using an intra-cavity electro-optic modulator *Opt. Express* **18** 1667–76

[12] Iwakuni K, Inaba H, Nakajima Y, Kobayashi T, Hosaka K, Onae A and Hong F-L 2012 Narrow linewidth comb realized with a mode-locked fiber laser using an intra-cavity waveguide electro-optic modulator for high-speed control *Opt. Express* **20** 13769–76

[13] Hagemann C, Grebing C, Kessler J, Falke S, Lemke N, Lisdat C, Schnatz H, Riehle F and Sterr U 2013 Providing 10^{-16} short-term stability of a 1.5 µm laser to optical clocks *IEEE Trans. Instrum. Meas.* **62** 1556–62

[14] Inaba H, Hosaka K, Yasuda M, Nakajima Y, Iwakuni K, Akamatsu D, Okubo S, Kohno T, Onae A and Hong F-L 2013 Spectroscopy of ^{171}Yb in an optical lattice based on laser linewidth transfer using a narrow linewidth frequency comb *Opt. Express* **21** 7891–6

[15] Nicolodi D, Argence B, Zhang W, Targat R L, Santarelli G and Coq Y L 2014 Spectral purity transfer between optical wavelengths at the 10^{-18} level *Nat. Photon.* **8** 219–23

[16] Leopardi H, Davila-Rodriguez J, Quinlan F, Olson J, Sherman J A, Diddams S A and Fortier T M 2017 Single-branch Er:fiber frequency comb for precision optical metrology with 10^{-18} fractional instability *Optica* **4** 879–85
[17] Häfner S, Falke S, Grebing C, Vogt S, Legero T, Merimaa M, Lisdat C and Sterr U 2015 8×10^{-17} fractional laser frequency instability with a long room-temperature cavity *Opt. Lett.* **40** 2112–5
[18] Matei D G *et al* 2016 A second generation of low thermal noise cryogenic silicon resonators *J. Phys.: Conf. Ser.* **723** 012031
[19] Cole G D *et al* 2016 High-performance near- and mid-infrared crystalline coatings *Optica* **3** 647–56
[20] Takamoto M, Takano T and Katori H 2011 Frequency comparison of optical lattice clocks beyond the Dick limit *Nat. Photon.* **5** 288–92
[21] Grebing C, Al-Masoudi A, Dörscher S, Häfner S, Gerginov V, Weyers S, Lipphardt B, Riehle F, Sterr U and Lisdat C 2016 Realization of a timescale with an accurate optical lattice clock *Optica* **6** 563–69
[22] Hachisu H, Nakagawa F, Hanado Y and Ido T 2018 Months-long real-time generation of a time scale based on an optical clock *Sci. Rep.* **8** 4243
[23] Pizzocaro M, Thoumany P, Rauf B, Bregolin F, Milani G, Clivati C, Costanzo G A, Levi F and Calonico D 2017 Absolute frequency measurement of the $^1S_0 - ^3P_0$ transition of ^{171}Yb *Metrologia* **54** 102
[24] Clivati C *et al* 2017 A VLBI experiment using a remote atomic clock via a coherent fibre link *Sci. Rep.* **7** 40992
[25] Tarallo M G, Calonico D, Levi F, Barbiero M, Lamporesi G and Ferrari G 2017 A strontium optical lattice clock apparatus for precise frequency metrology and beyond *Proc. of the 2017 Joint Conf. of the European Frequency and Time Forum and IEEE Int. Frequency Control Symp. (Besancon, 9–13 July 2017)* pp 748–50
[26] Telle H R, Lipphardt B and Stenger J 2002 Kerr-lens, mode-locked lasers as transfer oscillators for optical frequency measurements *Appl. Phys.* B **74** 16
[27] Rolland A, Li P, Kuse N, Jiang J, Cassinerio M, Langrock C and Fermann M E 2018 Ultra-broadband dual-branch optical frequency comb with 10^{-18} instability *Optica* **5** 1070–7
[28] Pizzocaro M, Costanzo G A, Godone A, Levi F, Mura A, Zoppi M and Calonico D 2012 Realization of an ultrastable 578 nm laser for an Yb lattice clock *IEEE Trans. Ultrason. Ferroelectr. Freq. Control* **59** 426–31
[29] Rauf B, Vélez López M C, Thoumany P, Pizzocaro M and Calonico D 2018 Phase noise cancellation in polarisation-maintaining fibre links *Rev. Sci. Instrum.* **89** 033103
[30] Clivati C, Mura A, Calonico D, Levi F, Costanzo G A, Calosso C E and Godone A 2011 Planar-waveguide external cavity laser stabilization for an optical link with 10^{-19} frequency stability *IEEE Trans. Ultrason. Ferroelectr. Freq. Control* **58** 2582–7